Vibrational Spectroscopy 104 (2019) 102945

Contents lists available at ScienceDirect

Vibrational Spectroscopy

journal homepage: www.elsevier.com/locate/vibspec

# Investigation of ostrich oil via Raman and infrared spectroscopy and predictions using the DFT method

Q.S. Martins[a,b,*], P.V. Almeida[a], Q.S. Ferreira[a], A. Oliveira[a], C. Aguirre[b], J.L.B. Faria[b]

[a] Departamento de Física, Universidade Federal de Rondônia, UNIR, Ji-Paraná, Brazil
[b] Instituto de Física, Universidade Federal de Mato-Grosso, Cuiabá, Brazil

ARTICLE INFO

*Keywords:*
Ostrich oil
Fatty acids
Raman spectroscopy
FTIR
DFT-calculation

ABSTRACT

Ostrich oil (OA) containing omega-3, 6, 9, was used to obtain vibrational signatures via Raman and Fourier transform infrared spectroscopy, comparing the results generated by ab initio calculations, following a qualitative transversal approach. The density functional theory (DFT) model, whose molecular geometries were based on the B3LYP functions with the 6-311G basis set, performed by GAUSSIAN 09 packages, was chosen due it is widely used for calculations involving organic compounds. The symmetries, vibrational assignments and calculations of the potential energy distribution (PED) were done using vibrational energy distribution analysis (VEDA) software. A bibliographical approach, based on typical samples, such as oleic, palmitic, linoleic, palmitoleic, stearic and linolenic acids (fatty acids), was submitted to the theoretical stage. The results, experimental (FTIR/Raman) and calculated spectra (CS) showed modes in the regions between 1400 and 1800 $cm^{-1}$, directly related to C = O and C = C belonging to carbon chains and in the range 3300–3500 $cm^{-1}$, related to the OH stretching modes. The modes showed a good approximation of the composition of the material, for both FTIR/Raman and CS, therefore justifying to the use of the methodology to certify the vibrational signature of the sample.

## 1. Introduction

The physical and chemical properties of oil are mainly related to its composition of fatty acids (FA) and degree of unsaturation. FA are organic substances found in solid or semi-solid (fats) and liquid phases belonging to the carboxylic acid group, compounds that have carboxyl, carbon double bonded to oxygen and hydroxyl groups. The difference between fat and oil is the physical state at room temperature, where fats contain more highly saturated fatty acids, and liquids unsaturated ones [1,2]. FA represent the predominant component of ostrich oil, with a lipid content of 98.8% from subcutaneous adipose tissue and 98.0% from retroperitoneal adipose tissue. Also described as polyunsaturated fatty acids (PUFA's), several studies correlate their therapeutic effects (anti-inflammatory, antibacterial and antifungal) with their ability to modify cell membrane phospholipids, modify cellular functions, and play a protective role for normal tissues [3]. Recently, in commercial research, oleic (omega-9), linoleic (omega-6) and linolenic (omega-3) acids were recognized as essential fatty acids. They represent products of commercial interest, containing certain vitamins and amino acids that help; for example, in the salubrity of the skin membranes, used as a mediator in combination with various medicinal or cosmetic ingredients to transport them below the skin barrier [2,3], among other benefits [4–7]. Majewsk [8] and others authors [9–13] have cited oleic, palmitic, and linoleic acids as the most abundant in concentrations of ostrich oil, and in smaller quantities palmitoleic, stearic, and linolenic acids. In this work, FTIR and Raman spectroscopy was used for the characterization of ostrich oil. Both are spectroscopic vibrational techniques for studying vibrational transitions in molecules. First, in FTIR spectroscopy, the samples are irradiated with IR light. The vibrational state is reached when part of the IR light is absorbed by the molecules, but only vibrations resulting in changes in the dipole moment of a molecule can absorb the IR radiation. A dipole is the product of charge (positive and negative) and distance. The last is a physical–chemical technique that shows the effects of the molecular polarization tensor in order to present its respective vibrational patterns. The technique has been widely applied for presenting fast and safe results, as it does not require any sample preparation and is easily applied to non-crystalline materials [14–16]. The Raman spectra were compared with ab initio calculations using DFT for the components presented. Thus Raman, as well as others [17–21], can be combined with chemometric methods, providing a good approach to the analysis of several materials [22–27]. The results obtained allowed presenting a spectral

* Corresponding author at: Departamento de Física, Universidade Federal de Rondônia, UNIR, Ji-Paraná, Brazil.
*E-mail address:* quesle@fisica.ufmt.br (Q.S. Martins).

https://doi.org/10.1016/j.vibspec.2019.102945
Received 1 April 2019; Received in revised form 22 July 2019; Accepted 23 July 2019
Available online 29 July 2019
0924-2031/ 

pattern or vibrational signatures for the ostrich oil and could be combined with an investigation about the general nature of FA. In the DFT calculations, the base was 6311G for the B3LYP functional, contributing to the processes of identification of the chemical nature, without prejudice to other identification methods or other bases. The results obtained showed a spectral pattern of vibrational signatures for the ostrich oil, exhibiting affinities with the general nature of the FA. Modes related to the O–H, C–H, and C = C bonds are well defined and may correspond to the molecules of flavons, polyphenols, and heptadecanoic, stearic, ecosanoic, palmitic, and palmitoleic acids, as well as omegas 3, 6 and 9.

## 2. Material and methods

The ostrich oil, sample came from Rondônia-Brazil in the microregion of Ji-Paraná was provided by Amazon Struthio, considering the necessary and essential procedures for preserving the quality of the material. For sample analysis, Raman and FTIR spectroscopy, and DFT as an analytical method were used.

### 2.1. Raman and FTIR spectroscopy

Confocal laser scanning microscopy (CLSM) was used on Horiba Xplora Series Raman equipment, spectral range from 0 to 4000 $cm^{-1}$, single laser 532 nm, confocal imaging 0.5 µm XY at high resolution. FTIR was carried out on an IRPrestige-21 Shimadzu Fourier transform infrared spectrophotometer with a resolution of 4 $cm^{-1}$, accumulation of 1 min, in the region of 2100 $cm^{-1}$ with a reading range of 0–4000 $cm^{-1}$.

### 2.2. DFT calculations

The molecular calculations were performed according to the density functional theory (DFT) model, whose molecular geometries were based on the B3LYP function with set 6-311G [26–28] in GAUSSIAN 09 packages [29]. PED calculations were carried out with the aid of the VEDA 4 program [32]. DFT was used to obtain the optimized structure of the compound, and its harmonic energy and vibrational frequencies were calculated with a hybrid three-parameter function (B3) used for the exchange part and Lee-Yang-Parr (LYP) functional correlation (a functional correlation that has local and nonlocal terms). The LYP correlation function is accepted as the most cost-effective approach for calculating the molecular structure, vibrational frequencies, and energy of optimized structures [25–31]. The symmetries, vibrational assignments, and calculations of the potential energy distribution (PED) were done with a high degree of accuracy. VEDA optimizes the set of internal coordinates for the development of IR/Raman experimental/theoretical systems. The results are represented by internal coordinates, giving users an overview of the use of multiple directions [33–38].

## 3. Results and discussion

### 3.1. FTIR analysis

After the experimental readings, it was observed in Fig. 1 that the 722 $cm^{-1}$ band can correspond to the bending of the –$(CH_2)n$–HC = CH group, as well as the C–O stretching [39–41]. The presence of the peak in Fig. 2 correspond to the C–C stretching [42]. The existence of this peak indicates the presence of long carbon chains and point out a sample characteristics. The peaks at 1095 and 1118 $cm^{-1}$ (Fig. 1) correspond to the stretching of CO, while the peak at 1745 $cm^{-1}$ is the stretching of C = O [43]. The peaks previously mentioned at 722, 1095, and 1118 $cm^{-1}$ represent the vibrations of omega-3 (linolenic acid), omega-6 (linoleic acid), and omega-9 (oleic acid). The 1160 $cm^{-1}$ peak represents the flavone, polyphenol, heptadecanoic, stearic, ecosanoic, pentadecanoic, myristic, palmitic, and palmitoleic acid vibrations in

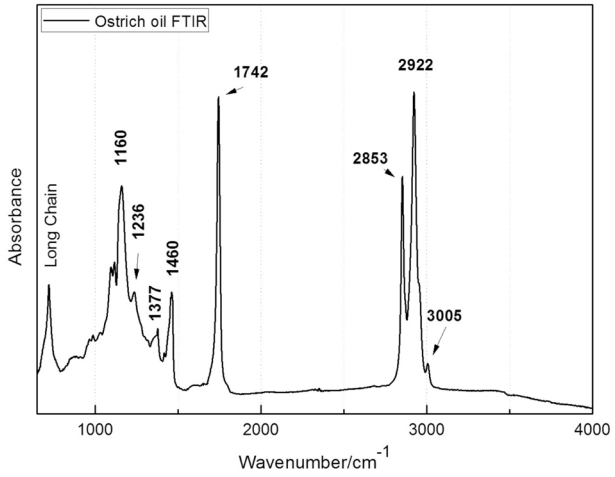


**Fig. 1.** Experimental FTIR of pure ostrich oil.

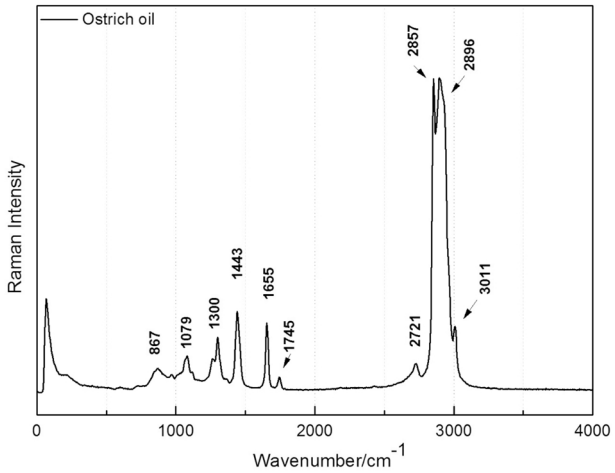


**Fig. 2.** Pure ostrich oil Raman spectrum.

addition to the previously mentioned omegas-3, 6, and 9. The peaks at 1378 and 1467 $cm^{-1}$ (Fig. 1) correspond to the bending of the methyl and methylene groups (CH groups), and the peaks at 1650 $cm^{-1}$ to C = C and 1744 $cm^{-1}$ (1742 $cm^{-1}$) (Fig. 1) to the stretching of C = O. Since C = O is a strong absorbent, we see that C = C absorbs much less, but with extra-close bands, that overlapping such a band mainly in the IR spectrum, due to bond symmetry. In this particular case, the C = C mode appears at the base of the band of C = O, practically hidden in the analysis. The spectra show a strong C–H vibrational mode between 3000 and 2850 $cm^{-1}$. Fig. 1 clearly shows separate bands corresponding to asymmetric C–H stretching at 2929 $cm^{-1}$ and symmetrical C–H stretching at 2856 $cm^{-1}$. Typically, OH absorption bands can be observed in the 3800–3200 $cm^{-1}$ stretching region. On the other hand, we can see that this region has no absorbance pattern and remains unchanged, due to oxidative conditions, which strongly depend on the nature of the sample. In both Figs. 1 and 2, this expected mode is not observed. On the other hand, in theoretical terms (Fig. 5), this mode is visible, suggesting its existence. The peaks at 2853, 2922, and 3005 $cm^{-1}$ correspond to the C–H, $CH_2$, and $–CH_3$ stretches, respectively. Finally, there is at peak at 3003 $cm^{-1}$ in Fig. 1 is related to a cis double bond and stretching of = C–H [39,40,44]. The vibrational patterns observed in Fig. 1 can be compared with Fig. 2. As complementary techniques, the adopted procedure can validate the mode set in each technique. Important bands can be detected, for example C = O (1650–1745 $cm^{-1}$), OH (2800–3200 $cm^{-1}$) and long-chain carbon bands, which break down below 750 $cm^{-1}$ in IR.

### 3.2. Raman analysis

Fig. 2 presents a characteristic spectrum of pure ostrich oil in the region between 867 and 1745 $cm^{-1}$, since that it is composed of long carbonic chains. Linolenic, linoleic, and oleic acids are some of the acids present in the sample (in Fig. 5. At 2721, 2857, 2896, and 3011 $cm^{-1}$ the modes stand out in very typical form and intensity for vegetable oils. This way, with intense and overlapped, fine and medium peaks, 2857 and 2896 $cm^{-1}$ exhibits the convolution of the $CH_2$, $CH_3$ and OH groups. They are very close to those observed in Fig. 2, but differ in intensity, possibly related to the means of observation, one considered an ideal medium, which is not true. Thus, because of the amorphous form of the material, the form at the base of the modes and the intensities may take different forms due to other forces or interactions with the environment.

Peaks at 867, 1079, 1300, 1433, 1655, and 1745 $cm^{-1}$ (Fig. 2) are present in common Raman spectra and can be found in almost all edible vegetable oils. Huang (2016), studying olive, peanut, and corn cooking oil, points out eight of these peaks and suggests that in Raman spectroscopy different oils and fats have only a small difference in relative peak intensity at 1654, 1265, and 970 $cm^{-1}$. Reference values (circles) were indicated to identify a linear correlation, which is shown in Fig. 3. The results presented in the Raman spectra, which in a simple way show us the nature of the ostrich oil in a relative pattern and analog of other oils. An analogy is can be seen for the 1745 and 1742 $cm^{-1}$ peaks, exhibiting stretching vibrations of the ester bond carbonyl, and still at 1655–1300 $cm^{-1}$ there are cis (C=C) and cis (CH) groups of unsaturated fatty acid and the peak at 970 $cm^{-1}$, which is related to trans-bending vibration (C=C) [28]. In this condition, Raman and IR bands show a clear change in intensity, and due to this we can indicate the vibrational selection factor for the type of technique. One is based directly on the variation of the induced dipole, while the other selects the vibrational modes based on the variation of molecular polarizability. Of course we may have similar, absent or displaced bands for a respective sample.

### 3.3. Calculated spectra

In Fig. 4, the set of calculated spectra (CS) have similar vibrational modes. This is observed due to the similar nature of the molecules, attributed to long carbon chains (Table 1), differentiated precisely by the difference in the presence of C=C.

For the CS results, the standard for the glycerol (**G**) molecule

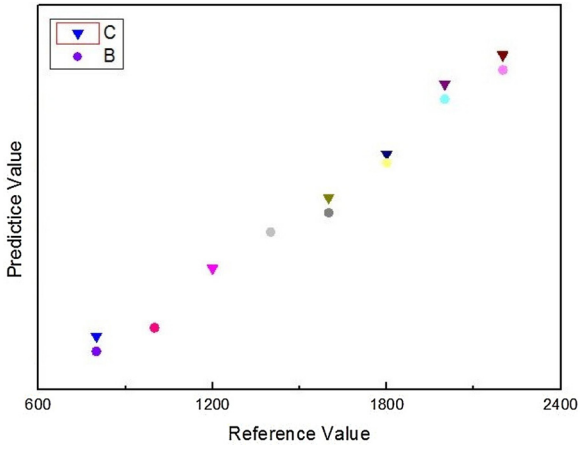


**Fig. 3.** Fitting for our results ($\alpha$ = experimental/theoretical – stars) and other experimental results ($\beta$ = reference values – circles) oils of different nature. $Y = a + bx$, with $a = 322.294$, $b = 0.64$. In this case, the adjustments are compared with more expressive results for analysis of vegetable oils observed in the literature with ostrich oil. See the comparison between two lines.

presenting the base formation fragment of the FA molecules is also shown. The importance of presenting the calculation for glycerol is precisely to understand the formation of vibrational modes when they contain the hydroxyls present in the chemical formation for the calculated components. CS comprise the region from 0 to 4000 $cm^{-1}$ with the main modes appearing between 1400 and 2000 $cm^{-1}$ and between 2800 and 3250 $cm^{-1}$. It can be seen that the mode at 3641 $cm^{-1}$ and 3637 $cm^{-1}$ is a symmetrical stretch-type vibration of the OH, a characteristic linkage of the FA. For glycerol, this vibration occurs at 3740 $cm^{-1}$ with symmetrical stretching and at 3700 $cm^{-1}$, asymmetric stretching for the OH at the opposite ends of the molecule, and between 1500 and 2000 $cm^{-1}$, the absence of some modes may be related to C=C bonds, mainly in bands around 1650 $cm^{-1}$. For A, B, C, and D, mean intensities of C=O bonds are 1720 $cm^{-1}$, which can be observed at very low intensity for E and F. At 1525 $cm^{-1}$, we see the angular CH deformations within the molecules. Still, for the main components except G, we see the active modes at 1340, 1325, 1155, 1105, and 1075 $cm^{-1}$. In the region of 2900–3050 $cm^{-1}$, asymmetric stretch type vibrations for CH are exhibited for all components. Table 2 presents data from the theoretical process, but emphasizes the molecules of oleic, linoleic and linolenic acid (omegas 9, 6 and 3), whose structures are shown in Fig. 5 since they are the major constituents of ostrich oil.

In assessing these results, it should be borne in mind that the modes of C=O and C–O (carboxylic acids) are well defined, and are in the region of 1720 $cm^{-1}$ and 1087 $cm^{-1}$, except for omega 6, at 1713 $cm^{-1}$ and 1146 $cm^{-1}$. The modes caused by the C=C conjugate stretches generally appear as a small intensity shoulder alongside the carboxyl, between 1700 and 1715 $cm^{-1}$, which is true for the calculated cases of omega 9 and 6. In Figs. 1 and 2, C=C appears quite discreetly at the base of the peak at 1742 $cm^{-1}$. It can be seen that in Fig. 5 this information is hidden at the base of the spectra but is shown at its respective frequencies after DFT analysis. Among the aspects presented in the region 1320–1420 $cm^{-1}$, the lower intensity modes are the representations for the vibrations of the –CH bonds along the molecule, usually of the twisting type. In Table 2, DFT data suggest vibrational modes in two general aspects: bending ($\delta$) and stretching ($\nu$). The contributions such as these vibrations are made are from the values calculated under the same potential energy distribution (PED), which appears in the signatures column. The minimum difference for these frequencies, or the absence of them, shows that the method is also valid for understanding the signatures of the components. It can be seen that for the calculated components, the optimization given by the maximum energy parameter (EPM), for oleic (EPM = 25.721), linoleic (EPM = 30.888), and linolenic acid (EPM = 31.078), is related to the size of the molecule [38]. The types of vibrations may vary for the cases mentioned, and this is closely linked to the energy received. However, these vibrational variations are minimized in the scope of this study. A good study on the subject can be found in other work [45]. Still, in Table 2, other vibrational contributions appear and are indicated by *S + number*. For the band at 1530 $cm^{-1}$ (omega 9), we have S59, S69, and S83, respectively, contributions of lower percentage of PED appearing for the same molecular group, vibration harmonic. Table 2 presents a summary format for presentation. A more complete view can be accessed in the supplementary material, Table S1.

## 4. Conclusions

The results of Raman/FTIR spectroscopy combined with ab initio calculations show ostrich oil vibrational bands. Differences found in the spectra may be related to the presence of C=C for the different components of the oil. Different intensities for carboxylic groups are verified, an indication of the form of activation of these vibrational modes according to the experimental technique used. In the experimental spectra, for example, the significant displacement of C=O (1720 $cm^{-1}$), may be due to the morphological relationships of the sample itself. As calculated, C=O appears at 1721 $cm^{-1}$ for oleic and

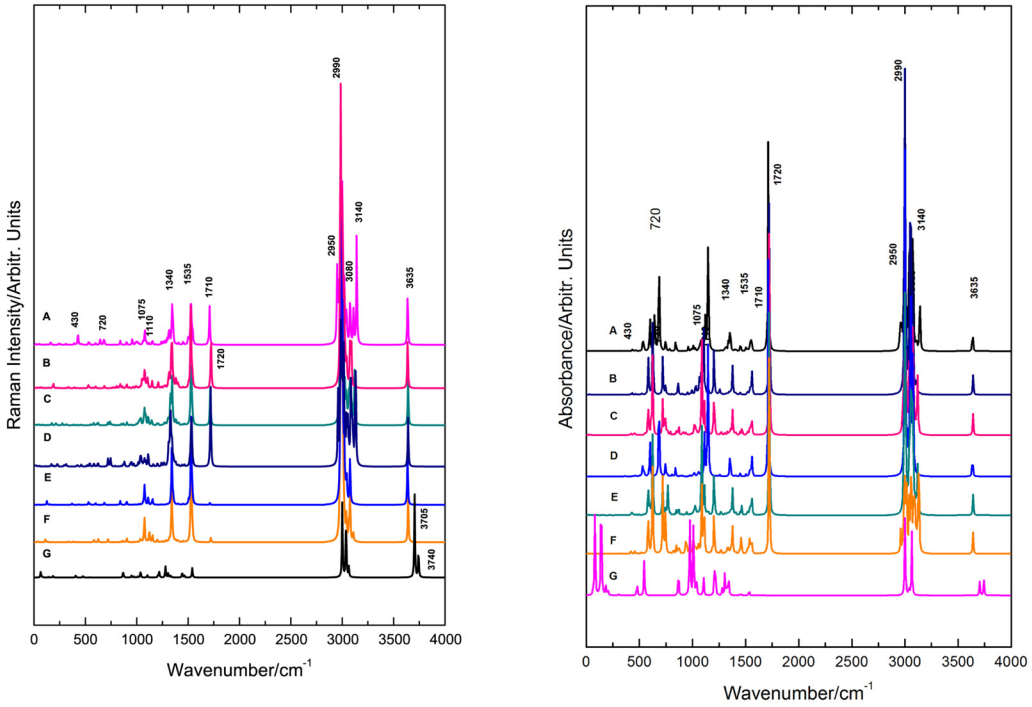


**Fig. 4.** DFT theoretical results B3LYP/6311G; Raman (left) and IR (right). (A) Linoleic; (B) Oleic; (C) Palmitoleic; (D) Linolenic; (E) Palmitic; (F) Stearic and (G) Glycerol.

linoleic acid. Between 750 and 1750 $cm^{-1}$ and between 2896 and 3011 $cm^{-1}$ the present modes are not distinguishable as to the origin of the sample, whether vegetable or animal. The DFT results helped to understand the behavior of the main components of the sample. Raman spectroscopy and FTIR were satisfactory and complementary to the characterization.

## Authors contributions

All the authors were involved in the preparation of the manuscript. All the authors have read and approved the final manuscript.

**Table 1**
Fatty acids and of ostrutch oil.

| FA's | Carbon numbers | Symbol |
|---|---|---|
| Palmitic | C16:0 | E |
| Palmitoleic | C16:1 | C |
| Stearic | C18:0 | F |
| Oleic (omega 9) | C18:1 | B |
| Linoleic (omega 6) | C18:2 | A |
| Linolenic (omega 3) | C18:3 | D |

The symbolism given links the results of Fig. 4.

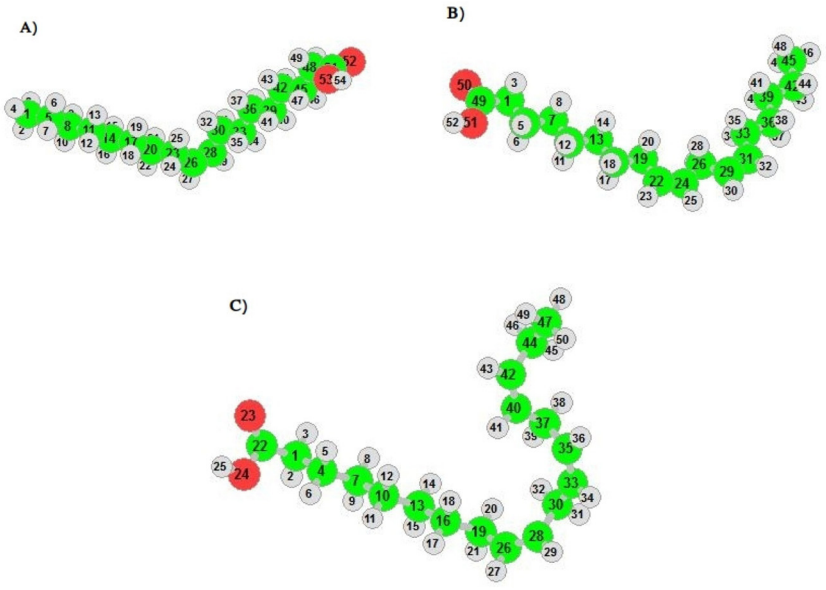


**Fig. 5.** Structure fatty acids. (a) Oleic acid (b) Linoleic acid (c) Linolenic acid for all structure (green-carbon), (red oxygen) and white hydrogen.

**Table 2**
General patterns of vibrational behavior for calculated values for omega 9, 6 and 3 molecules.

| Component | $\omega$/cm$^{-1}$ | | Assignment of the molecular | Other PED |
|---|---|---|---|---|
| | *Raman* | *FTIR* | | |
| | 1344 | | δ(HCC)(21 20 23) [14] | |
| | 1464 | 1464 | δ(HCC)(27 26 28) [41] | S73 |
| | 1527 | | δ(HCH)(38 36 37) [42] | S63, S77, S81 |
| | 1530 | | δ(HCH)(10 8 9) [19] | S59, S69, S83 |
| Omega 9 | | 1557 | δ(HCH)(41 39 40) [22] | S79, S83, S85 |
| | 1713 | 1713 | ν(C=C)(28 26) [72] | |
| | 1721 | 1721 | ν(C=O)(52 51) [78] | |
| | 2989 | | ν(CH)(20 22) [17] | S5, S6, S11, S12 |
| | | 2998 | ν(CH)(33 34) [40] | S5, S7, S10, S13, S16, S26, S27 |
| | | 3122 | ν(CH)(28 29) [49] | S19 |
| | 3641 | 3641 | ν(OH)(53 54) [100] | |
| | 1078 | 1078 | ν(CC)(13 16) [31] | S44, S45, S47 |
| | 1093 | 1093 | ν(CC)(1 4) [23] | |
| | 1317 | 1317 | δ(HCC)(25 24 26) [14] | |
| | | 1556 | δ(HCH)(11 10 12) [29] | S56, S60, S64, S66 |
| | 1709 | 1709 | ν(C=C) (24 22) + (29 31) [39] | S35 |
| Omega 6 | 1713 | 1713 | ν(C=O)(50 49) [79] | |
| | 2957 | 2957 | ν(CH)(26 27) + (26 28) [48] | |
| | 3007 | 3007 | ν(CH) (45 47) + (45 48) [37] | S8, S9, S12, S13, S30 |
| | 3141 | 3141 | ν(CH)(24 25) [35] | S7, S16, S17 |
| | 3637 | 3637 | ν(OH) (51 52) [100] | |
| | 948 | 948 | ν(CC)(30 28) [16] | |
| | 1055 | 1055 | ν(CC)(30 28) [13] | S37, S43 |
| | 1202 | 1202 | δ(HOC)(25 24 22) [24] | |
| | 1441 | 1441 | δ(HCH)(49 47 48) [26] | S71, S77, S79 |
| Omega 3 | 1535 | 1535 | δ(HCH)(46 44 45) [33] | S74, S79 |
| | 1720 | 1720 | ν(C=C) (28 26)[11] + (35 33)[38] + (42 40)[23] | |
| | 1721 | 1721 | ν(C=O) (23 22) [78] | |
| | 2959 | 2959 | ν(CH)(30 31) [98] | |
| | | 2998 | ν(CH)(16 17) [36] | S8, S11 |
| | 3133 | 3132 | ν(CH) (35 36) [54] | S21 |
| | 3641 | | ν(OH) (24 25) [100] | |

Here are presented the more general natures of vibrations, these being able to have specific variations according to the type movements of the atoms. Bending ($\delta$) and stretching ($\nu$).

## Acknowledgements

The authors would like to give thanks to Amazon Struthio for the sample assigned to this study, to the Grupo de Optica e Nanoscopia (GON) and Laboratorio de Caracterização e Microscopia de Materiais (LCMMAT) of the Universidade Federal de Alagoas, to the research group Estrutura da Matéria e Física Computacional/DEFIJI/UNIR and FAPERO/CAPES (Grant number: 008/2018).

## Appendix A. Supplementary data

Supplementary data associated with this article can be found, in the online version, at https://doi.org/10.1016/j.vibspec.2019.102945.

## References

[1] R.D. O'Brien, AOCS Press, 2nd ed., 2000.
[2] S. Gavanji, B. Larki, A. Hosein, J. Novel Appl. Sci. 18 (2013) 650–654.
[3] H. Ali, H. Nawaz, M. Saleem, F. Nurjis, M. Ahmed, J. Raman Spectrosc. 47 (2016) 706–711.
[4] W. Dong, Y. Zhang, B. Zhang, X. Wang, J. Raman Spectrosc. 44 (2013) 1739–1745.
[5] J.O. Horbańczuk, I. Malecki, R.G. Cooper, A. Jóźwik, J. Klewiec, J. Krzyżewski, H. Khalifa, W. Chyliński, A. Wójcik, M. Kawka, Anim. Sci. Pap. Rep. 22 (2004) 247–251.
[6] V. Baeten, P. Hourant, M.T. Morales, R. Aparicio, Agric. Food Chem. 44 (1996) 2225–2230.
[7] U.D. Palanisamy, M. Sivanathan, A.K. Radhakrishnan, N. Haleagrahara, T. Subramaniam, G.S. Chiew, Molecules 16 (2011) 5709–5719.
[8] D. Majewska, D. Szczerbińska, M. Ligocki, M. Buclaw, A. Sammel, Z. Tarasewicz, K. Romaniszyn, J. Majewski, J. Brit. Poult. Sci. 57 (2016) 193–200.
[9] X. Liu, F. Wang, X. Liu, Y. Chen, L. Wang, Eur. J. Lipid Sci. Technol. 113 (2011) 775–779.
[10] D. Majewska, J. Brit. Poult. Sci. (2016) 57.
[11] D. Belichovska, Z. Hajrulai-Musliu, R. Uzunov, K. Belichovska, M. Arapcheska, Mac. Vet. Rev. 38 (2015) 53–59.
[12] P. la Mataa, A. Dominguez-Vidalb, J.M. Bosque, S.A. Ruiz, M.L. Cuadros, R.M.J. Ayora, Food Control 23 (2012) 449–455.
[13] H. Yanga, J. Irudayaraj, M.M. Paradkarb, Food Chem. 93 (2005) 25–32.
[14] T. De Beer, A. Burggraeve, M. Fonteyne, L. Saerensa, J.P. Remon, C. Vervaet, Int. J. Pharm. 30 (1-2) (2011) 32–47 417, doi: 10.1016/j.ijpharm.2010.12.012.
[15] C.B. Silva, J.G. da Silva Filho, G.S. Pinheiro, A.M.R. Teixeira, P.T.C. Freire, Vibrat. Spectrosc. 98 (2018) 128–133, https://doi.org/10.1016/j.vibspec.2018.08.001.
[16] A. Abkari, I. Chaabane, K. Guidara, Physica E 81 (2016) 136–144, https://doi.org/10.1016/j.physe.2016.03.010.
[17] X.F. Zhang, M.Q. Zou, X.H. Qi, F. Liu, C. Zhang, F. Yin, J. Raman Spectrosc. 42 (2011) 1784–1788.
[18] H. Sadeghi-Jorabchi, P.J. HendraR, H. Wilson, P.S. Belton, J. Am. Oil Chem. Soc., 67, 483–486.
[19] H. Yanga, J. Irudayaraj, M.M. Paradkarb, Food Chem. 93 (2005) 25–32.
[20] G.F. Ghesti, J.L. de Macedo, I.S. Resck, J.A. Dias, S.C. Dias, Energy Fuels 21 (2007) 2475–2480.
[21] P. Pavón, N. Sánchez, F. Laespada, M. Cordero, Anal. Bioanal. Chem. 394 (2009) 1463–1470.
[22] F.P. Capote, J.R. Jiménez, M.D. de Castro, Anal. Bioanal. Chem. 388 (2007) 1859–1865.
[23] H. Chena, M. Angiuli, C. Ferrari, E. Tombari, G. Salvetti, E. Bramantib, Food Chem. 125 (2011) 1423–1429.
[24] V. Baeten, Lipid Technol. 22 (2010) 36–38.
[25] A.D. Becke, J. Chem. Phys. 98 (1993) 5648.
[26] C. Lee, W. Yang, R.G. Parr, Phys. Rev. B 98 (1988) 785.
[27] X. Wu, S. Gao, J.S. Wang, H. Wang, Y.W. Huanga, Y. Zhaod, Analyst 137 (2012) 4226–4234.
[28] F. Huang, Y. Li, H. Guo, J. Xu, Z. Chen, J. Zhang, Y. Wang, J. Raman Spectrosc. 47 (2016) 860–864.
[29] M.J. Frisch, G.W. Trucks, H.B. Schlegel, G.E. Scuseria, M.A. Robb, J.R. Cheeseman, G. Scalmani, V. Barone, B. Mennucci, G.A. Petersson, H. Nakatsuji, M. Caricato, X. Li, H.P. Hratchian, A.F. Izmaylov, J. Bloino, G. Zheng, J.L. Sonnenberg, M. Hada, M. Ehara, K. Toyota, R. Fukuda, J. Hasegawa, M. Ishida, T. Nakajima, Y. Honda, O. Kitao, H. Nakai, T. Vreven, J.A. Montgomery, J.E. Peralta, F. Ogliaro, M. Bearpark, J.J. Heyd, E. Brothers, K.N. Kudin, V.N. Staroverov, R. Kobayashi, J. Normand, K. Raghavachari, A. Rendell, J.C. Burant, S.S. Iyengar, J. Tomasi, M. Cossi, N. Rega, J.M. Millam, M. Klene, J.E. Knox, J.B. Cross, V. Bakken, C. Adamo, J. Jaramillo, R. Gomperts, R.E. Stratmann, O. Yazyev, A.J. Austin, R. Cammi, C. Pomelli, J.W. Ochterski, R.L. Martin, K. Morokuma, V.G. Zakrzewski, G.A. Voth, P. Salvador, J.J. Dannenberg, S. Dapprich, A.D. Daniels, Ö. Farkas, J.B. Foresman, J.V. Ortiz, J. Cioslowski, D.J. Fox, Gaussian 09, (2009).
[30] B. Becke, Phys. Rev. B 38 (1998) 3098–3100.
[31] T.K. Kuruvilla, J.C. Prasana, S. Muthu, J. George, S.A. Mathew, Spectrochim. Acta Part A: Mol. Biomol. Spectrosc. 188 (2018) 382–393.
[32] M.H. Jamroz, Vibrational Energy Distribution Analysis, VEDA 4 Program, Warsaw, Poland, 2004.
[33] Y. Morino, K. Kuchitsu, J. Chem. Phys. 20 (1952) 1809–1810.
[34] W.J. Taylor, J. Chem. Phys. 22 (1954) 1780–1781.
[35] T. Miyazawa, T. Shimanouchi, S. Mizushima, J. Chem. Phys. 29 (1958) 611–616.
[36] G. Keresztury, G. Jalsovszky, J. Mol. Struct. 10 (1971) 304.
[37] P. Pulay, G. Fogarasi, F. Pang, J.E. Boggs, J. Am. Chem. Soc. 101 (1979) 2550–2560.
[38] M.H. Jamróz, Spectrochim. Acta Part A: Mol. Biomol. Spectrosc. 114 (2013) 220–230.
[39] N. Cebi, M.T. Yilmaz, O. Sagdic, H. Yuce, E. Yelboga, Food Chem. 225 (2017) 188–196 doi: 10.1016/j.foodchem.2017.01.013.
[40] M.D. Guillén, N. Cabo, J. Sci. Food Agric. 80 (2000) 2028–2036 doi.org/10.1002/1097-0010(200011)80:14 < 2028AID-JSFA713 > 3.0.CO;2-4.
[41] N.E. Maurer, B. Hatta-Sakoda, G. Pascual-Chagnan, L.E.R. Saona, Food Chem. 134 (2012) 1173–1180 doi: 10.1016/j.foodchem.2012.02.143.
[42] K. Malek, E. Podstawka, J. Milecki, C. Schroeder, L.M. Proniewicz, Biophys. Chem. 142 (2009) 17–26 doi.org/10.1016/j.bpc.2009.02.007.
[43] B. Innawong, P. Mallikarjunan, J. Irudayaraj, J.E. Marcy, Food Sci. Technol. 37 (2004) 23–28 doi.org/10.1016/S0023-6438(03)00120-8.
[44] A. Rohaman, Y.B. Che Man, Sci. World J. (2012) 2012, https://doi.org/10.1100/2012/250795.
[45] P. Lark, Infrared and Raman Spectroscopy: Principles and Spectral Interpretation, Elsevier, 2011.